Medical Sciences

Interaction of expanding abdominal aortic aneurysm with surrounding tissue: Retrospective CT image studies

Sebastian T. Kwon[1], William Burek[2], Alexander C. Dupay[2], Mehdi Farsad[2], Seungik Baek[2,*], Eun-Ah Park[3], and Whal Lee[3]

[1]University of Michigan Medical School, 1500 East Medical Center Drive, Ann Arbor, MI 48109, USA. [2]Cardovascular and Tissue Mechanics Research Laboratory, Michigan State University, 2555 Engineering Building, East Lansing, MI 48824, USA. [3]Department of Radiology, Seoul National University College of Medicine, 28 Yongon-dong, Jongno-gu, Seoul, Korea

***Objectives*: Abdominal aortic aneurysms (AAA) that rupture have a high mortality rate. Rupture occurs when local mechanical stress exceeds the local mechanical strength of an AAA, so stress profiles such as those from finite element analysis (FEA) are useful. The role and effect of surrounding tissues, like the vertebral column, which have not been extensively studied, are examined in this paper.**

***Methods*: Longitudinal CT scans from ten patients with AAAs were studied to see the effect of surrounding tissues on AAAs. Segmentation was performed to distinguish the AAA from other tissues and we studied how these surrounding tissues affected the shape and curvature of the AAA. Previously established methods by Veldenz et al. were used to split the AAA into 8 sections and examine the specific effects of surrounding tissues on these sections [1]. Three-dimensional models were created to better examine these effects over time. Registration was done in order to compare AAAs longitudinally.**

***Results*: The vertebral column and osteophytes were observed to have been affecting the shape and the curvature of the AAA. Interaction with the spine caused focal flattening in certain areas of the AAA. In 16 of the 41 CT scans, the right posterior dorsal section (section 5), had the highest radius of curvature, which was by far the section that had the maximum radius for a specified CT scan. Evolution of the growing AAA showed increased flattening in this section when comparing the last CT scan to the first scan.**

***Conclusion*: Surrounding tissues have a clear influence on the geometry of an AAA, which may in turn affect the stress profile of AAA. Incorporating these structures in FEA and G&R models will provide a better estimate of stress.**

***Clinical Relevance:* Currently, size is the only variable considered when deciding whether to undergo elective surgery to repair AAA since it is an easy enough measure for clinicians to utilize. However, this may not be the best indicator of rupture risk because small aneurysms also contribute to a high mortality rate. AAA's wall stress is a superior indicator and may be better predicted with the inclusion of these surrounding tissues, which then could be used by clinicians in their decision-making process on whether to operate on an AAA.** *Journal of Nature and Science, 1(8):e150, 2015*

Abdominal aortic aneurysm | Surrounding tissue | Longitudinal images | Growth and remodeling | Inscribed spherical diameters

INTRODUCTION

As an abdominal aortic aneurysm (AAA) enlarges, it becomes subject to increased reaction forces from surrounding tissue, which in turn becomes a factor of AAA growth and remodeling. Currently, medical professionals consider AAA's maximum cross sectional diameter as the ultimate indicator of rupture risk for a patient diagnosed with an AAA. If the maximum cross-sectional diameter exceeds 5.0 cm or 5.5 cm, surgical intervention is typically recommended. This criteria was developed to set a clear boundary where the risk of rupture becomes appreciably greater than the risks involved in surgery, which has mortality rates of up to 5.8% - 6% [2,3]. Statistically significant studies suggest early elective surgery in lieu of continued monitoring may not improve survival [3–5], but rupture of small AAAs is still responsible for high mortality rates [3,6]. Rupture of an AAA occurs due to mechanical failure when the wall stress exceeds its strength. Accordingly, finite element analysis (FEA) based on patient-specific AAA's geometry is capable of evaluating AAA's wall stress and it has been shown to be a better estimator of rupture risk than the maximum diameter criteria [7–10].

While most computational biomechanical studies typically involve the internal arterial pressure as the sole mechanical driving force affecting surface evolution, there have been growing suggestions emphasizing that the addition of a growth barrier, such as the vertebral column, would provide significant reaction forces to AAA. This would change the outcome of FEA based stress analysis, offering more insight as to the complex biomechanics in effect under *in vivo* conditions [11,12]. For instance, Vorp et al. suggest that the "limitation of posterior expansion caused by the vertebral column might result in preferential anterior expansion of the aneurysmal wall and an asymmetric configuration" [11]. Indeed, using a computational growth and remodeling (G&R) model, Watton et al. has demonstrated that a symmetric AAA grows to an asymmetric shape due to interaction with the spine [12]. Hence, it is feasible that the interactions with the aneurysmal wall can generate an adverse local elevation of the stress state, in which rupture potential increases and requires accurate prediction using FEM analysis. Nevertheless, there is no clear understanding of: which region in a growing lesion interacts with surrounding tissues, morphological features associated with interaction, and how significantly these features affect long term interaction and alteration. The objective of this study is, hence, to identify morphological features of AAA surface, which arise from AAA interaction with surrounding tissues.

Many research groups have reconstructed 3-D AAA geometries from CT scans with the aim of evaluating wall stress through computational biomechanics by using non-longitudinal patient-specific 3-D AAA geometries reconstructed from CT scans [7,13–25]. Studies including longitudinal data are, however, seriously underrepresented, as access to such data collections is rare, especially at high resolutions. Diagnosis and follow-up is typically done through the use of ultrasound imaging because it presents a cheaper and faster method than CT imaging, which is usually only utilized for surgical planning. However, longitudinal CT scan data not only allows for the investigation of morphological parameter values, but their evolution as well. Therefore, a set of longitudinal data provides a better understanding of the mechanism associated with AAA's rupture potential as well as a more accurate prediction of AAA's geometrical and biomechanical characteristics during expansion.

Morphological features, which are generated by/during AAA expansion and the resulting interactions, necessitate the use of longitudinal images. Therefore, registration based on the vertebral column allows for the observation of long-term temporal movement, expansion, and change of shape of the aorta to some absolute reference. In addition to the locally observable effects of the spine, it affects the overall AAA growth pattern, especially for

Conflict of interest: No conflicts declared.

* Corresponding Author. S. Baek, Ph.D. Department of Mechanical Engineering, 2457 Engineering Building, Michigan State University East Lansing, MI 48824, USA.
T: +1-517-432-3161; F: +1-517-353-1750.
Email: sbaek@egr.msu.edu

an aneurysm that preferentially grows posteriorly but presents anterior growth due to tissue constraints. The morphological features will lend insight into the link between AAA pathology and AAA biomechanics by being indicative of particular stress profiles, serving as a strong tool for computational biomechanics.

METHODS

This study was subject to Internal Review Board approvals at Seoul National University Hospital and Michigan State University. No patient consent was necessary since the data was collected during a retrospective study.

The demographic data for the longitudinal dataset obtained from Seoul National University Hospital is detailed in Table 1. Each patient is either under continued monitoring or has been subject to surgical intervention; there are no rupture cases in this study. Scans of patients who had undergone surgical intervention were excluded from this study. The data set of a patient E is not included in this study, because the patient exhibited only a thoracic aneurysm, as well as the final 2 scans from patient H and the final scan from patient K that appeared to be post-operative.

Table 1. Demographic patient data for the utilized longitudinal dataset. Age is stated for the initial scan.

Patient ID	A	B	C	D	F	G	H	I	J	K
Initial Age (years)	68	71	69	63	82	65	68	66	54	62
Gender	M	M	M	F	F	M	M	M	M	M
Scan Intervals (years)	0	0	0	0	0	0	0	0	0	0
	0.5	0.6	1.7	1.4	1.2	0.5	1.1	1.0	1.1	0.6
		2.0		3.7	4.0	1.0	5.8	2.0	2.1	1.8
					4.2	1.5	6.7	2.9	3.1	2.9
					4.7	2.0	7.7	3.9	3.5	3.8
					6.0	2.5	8.6	5.9		
					7.2		9.1			

To better understand the causes of rupture in AAAs, an analysis of the geometric evolution of the AAA of several patients was performed. Segmentation of lumen volumes and tissue volumes were produced. CT data files were processed using the biomedical imaging software, Mimics® (Materialise, Leuven, Belgium). For a given initial CT scan, a threshold intensity value range (> 226 Housefield Units (HU) – a measure of radiodensity) was selected to allow for clear viewing of the vessel boundary contours and was distinctly created by the presence of an intravenous contrast agent within the lumen volume. The vertebral column from each CT data file underwent thresholding in an identical manner (> 226 HU), but due to bone density variations, the range was expanded to ±75 HU for more accurate reconstruction for some patients. A threshold value was selected (> -25 HU), which captured arterial wall tissue and intraluminal thrombus layer (ILT) together, as there was no discernible density difference between the two. The inner boundary of the combined volume was equivalent to the lumen surface while the outer boundary underwent editing to properly differentiate it from surrounding tissue.

In order to properly study the three-dimensional aspect of the aneurysms, 3-D models of each tissue (i.e. veins, arteries, kidneys, spine) were produced using region growing and the 2-D masks from segmentation. These were generated using a subjective degree of Laplacian smoothing with a smoothing factor of 0.7 and a centerline approximation of the vessel was computed using the MedCad module within the Mimics imaging software package. A visual inspection of the models allowed for a quantitative analysis of flattening. Locations for analysis were chosen subjectively based on maximum global and local flattening of the AAA around vertebra L4. Proper divisions of the CT cross section of the aneurysm follow the methods established by Veldenz et al. [1]. In accordance with prior methodology, the aneurysm cross section was split into eight radial sections of 45° increments beginning with the (left) anterior ventral side, increasing in the clockwise direction. The naming of the sections and measurement method are shown in Figure 1. Two individuals generated the data using this method and the results were averaged and are presented below.

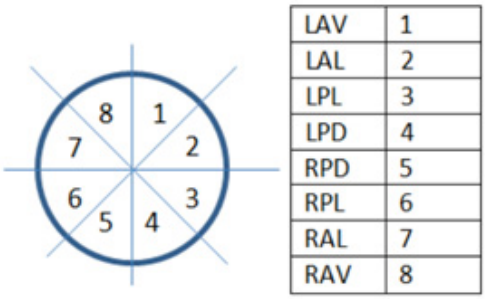

Figure 1. Methods established by Veldenz et. al; numerical section assignment of eight sections beginning with the left anterior ventral (LAV) section. (L=Left, R=Right; A=Anterior, P=Posterior; V=Ventral, L=Lateral, D=Dorsal.)

The center of the radii for the measurements were assigned by using the MedCad centerline approximation as the center point. The eight sections were then bisected by another angle at 22.5° to allow for three point approximations of circumscribed circles. The circumscribed circles were produced from the initial point, end point and the midpoint as seen in Figure 2. A curvature of radius measurement was performed using the MedCad module of the Mimics software and a set of eight curvature measurements was produced from each scan. Additionally qualitative information, including aneurysm contact type and location of contact point, were recorded. Using the measurement method, two evaluators independently made their measurements and the mean values of measurements were recorded.

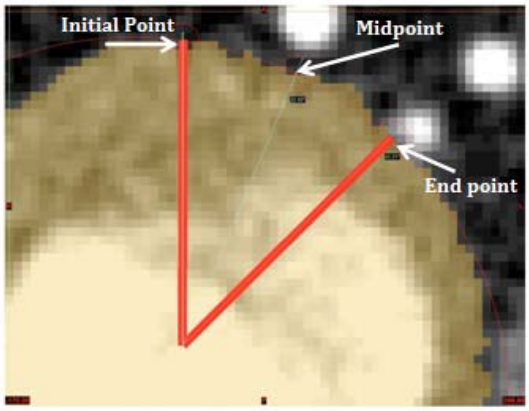

Figure 2. Measurement points for circumscribed circles for Patient J, Scan 2 at 1.1 years.

For a longitudinal study, it is necessary to remove differences in patient tissue positioning and location as interpreted through CT data between initial and follow-up scans to analyze the true spatial differences (displacement, growth, and remodeling) among respective models over time. An iterative global registration algorithm at 1,000 iterations with 80% subsample percentage was employed, which minimizes the total distance field between two stereolithography (STL) or 3-D models. The vertebral column was considered to be relatively unchanging and of constant shape and size over time, such that registering the vertebral column from a follow-up scan to the vertebral column from the respective initial scan is stable when compared to the series of AAAs shape evolution. Accurate alignments of the vessel models for a given patient from each available time-step are then attained by applying the resulting transformation matrix from vertebral registration to impose the same relative transformation on the vessel models. The result is, thus, that the sum of all the spatial changes to the vessel models over the available timeframe from displacement, growth,

and remodeling can be interpreted. One example of model registration is shown by Figure 3, which shows the relatively unchanging vertebral column.

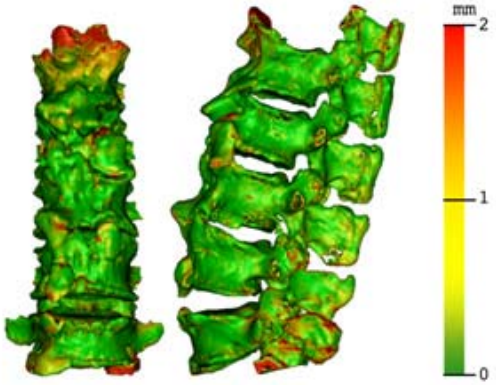

Figure 3. The absolute differences of the vertebral column from A2 registered to the vertebral column from A1 (This patient displays significant osteophytes). Left: anterior view of spine. Right: lateral view of spine.

Visual examination of the CT data concurrently with the generated 3-D models was performed to identify morphological features of AAAs influenced by surrounding tissue. In particular, two spatial regions were focused upon. The first spatial region was the upper infrarenal area consisting of the inferior vena cava (IVC), mesenteric artery networks, diaphragm, renal system, and celiac artery network. The second region was the vertebral column interaction with an AAA considering the tissue interface between the two. A representation of the aforementioned tissues is shown in Figure 4.

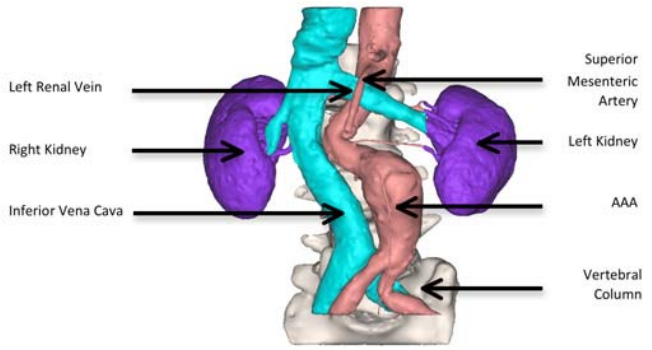

Figure 4. An example of STL models for AAA and surrounding tissues from scan B2

RESULTS

Results include STL models and radiographic images, which show the interaction with surrounding tissues, as well as the calculated radii of curvature for the CT scans. Table 2 summarizes the contact of the surrounding tissues (including osteophytes, spinal column, vena cava) with the aneurysm.

Upon observing overlapped images from the longitudinal CT scans, it appeared that some combination of the IVC, mesenteric artery networks, diaphragm, renal system, and celiac artery network do not alter the centerlines of the aorta in the upper infrarenal region of the aorta by partially, but effectively, anchoring the aorta at that location and above. In addition, the IVC was modeled using segmentation and the STL model for scan B2 was utilized to visualize its interactions with an AAA (Figure 4). The shape of the aorta deviated from standard anatomical position below the left renal vein. As the infrarenal aorta begins at the renal branches, it is clear that in the sequential scans, the tortuosity gradually increases as can be seen by a deviation of the centerline from the initial centerline [26]. Patients C and J do not support this trend as strongly as the others, but all vessels present some degree of tortuosity. This tortuosity is three-dimensional, as the same trend can be observed in the coronal and sagittal planes.

Table 2. Surrounding tissues contacting the aneurysm

Patient	Scan	Contact Regions	Type of Contact
B	1	5	Spine L4 (osteophyte)
	2	5, 6 partial	Spine L4 (osteophyte)
	3	4 partial, 5	Spine L4 (osteophyte)
C	1	4, 5	Spine L4 (osteophyte)
	2	4,5	Spine L4 (osteophyte)
D	1	4 partial, 5 partial	Spine L3
	2	4 partial, 5, 6	Spine L3 (4,5);Vena Cava (5,6)
	3	4, 5, 6 partial	Spine L3 (4,5 partial); Vena Cava (5, 6)
G	1	5	Spine L4
	2	5	Spine L4
	3	5	Spine L4
	4	4 partial, 5	Spine L4
	5	4 partial, 5	Spine L4
	6	4 partial, 5,6	Spine L4 (4,5);Vena Cava(6)
I	1	5, 6 partial	Spine L4 (osteophyte)
	2	5, 6 partial	Spine L4 (osteophyte)
	3	5, 6 partial	Spine L4 (osteophyte)
	4	5, 6	Spine L4 (osteophyte); Vena Cava (6)
	5	5, 6	Spine L4 (osteophyte); Vena Cava (6)
	6	5,6	Spine L4 (osteophyte); Vena Cava (6)
J	1	4 partial, 5 partial	Spine L4
	2	4 partial, 5	Spine L4
	3	4 partial, 5	Spine L4
	4	4 partial, 5	Spine L4
	5	4 partial, 5, 6 partial	Spine L4, Vena Cava(6)

It is difficult to differentiate the aneurysmal wall/ILT tissue from surrounding soft tissue. However, in this study we focused on external tissues affecting the AAA without regarding the ILT. Table 2 shows a summary of the interaction of AAA with surrounding tissues of the patients in the longitudinal data set of Table 1. Figure 6 shows the CT images that show the AAA flattening at the contact surface with the vertebral column.

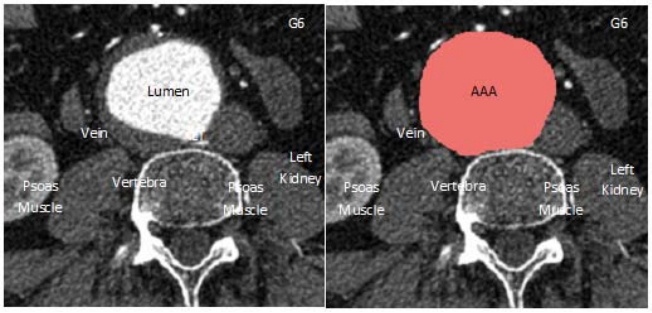

Figure 5. Pre- and post-segmentation of a representative CT image from G6 showing AAA interaction with the vertebral column.

Most of the patients in this study showed flattening of the AAA against the vertebral column, which is quantified by the radii of curvature shown in Figure 7. Section 5 (right posterior dorsal) more often than not showed the highest radius of curvature, meaning the AAA was the flattest in this region (Table 3). While this section was not the flattest for earlier scans, it was the flattest at the last CT scan, showing that growth of AAA leads to increased interaction with the spine at this location. However, the flattening of this region was not gradual with time; instead, the radius of curvature seemed to alternate in size every other scan. For example with patient G, the radius of curvature would alternate between large and small. Concordantly, the regions surrounding the flattened sections (4 and 6) become more and more rounded as time went on. The transitions between the sections with large radii of curvature to sections with smaller radii of curvature may be areas of stress concentration.

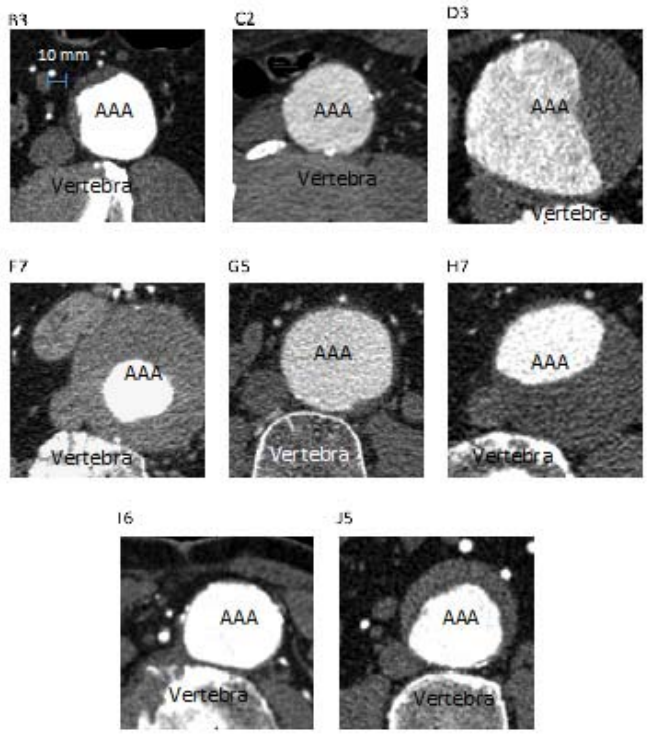

Figure 6. Zoomed in images of B3, C2, D3, F7, G5, H7, I6, J5. All cases are in contact with the upper half of the L4 vertebrae, except H7, which is documented for the upper half of the L3 vertebrae. The images have the same magnification with a scale of 10mm shown in scan B3.

Table 3. Analysis of R* by section

Section	Number of times specified section had:			
	Highest R* for a CT scan	Highest R* for the first CT scan for each patient	Highest R* for the last CT scan for each patient	R*>2
1	6	1	1	0
2	4	1	1	0
3	3	0	1	0
4	5	4	0	1
5	16	2	4	5
6	3	0	2	0
7	0	0	0	0
8	4	1	0	0

It is known that the vertebral column limits posterior expansion of an AAA. By comparing registered vessels from longitudinal images, it can be seen over time that the posterior side of the aneurysmal wall indeed experiences little to no change when compared to the rest of the lesion (Figure 8). Therefore, it appears that the vertebral column acts as a physical barrier to posterior growth of the AAA.

Severe ossification was observed in patients A, B, C, H, and I with a clear effect on the geometry of the respective AAAs (Figure 9). As osteophytes originate from the spinal column, the posterior aneurysmal wall was affected more than the anterior wall. It was also observed that osteophytes grow into the posterolateral region of the AAA as in patient A, creating a small indent at this location.
Figure 9. Ossification contact from patient A (A2)

DISCUSSION

Immediately upon visually reviewing the CT scans, the interaction between the vertebral column and the AAA is apparent. The patients studied displayed different degrees of interaction with surrounding tissues and for a subset of the patients, a marked effect on AAA geometry was observed. Interaction with the spine was prevalent and caused clear flattening of the AAA. On the other hand, interaction due to ossifications was more patient specific, because of its variability in prevalence. Some patients showed marked flattening of AAA against osteophytes while others with healthy spines had no such effects. Although in some segmented CT scans the AAA seemed to flatten against the IVC, it is thought that the relatively miniscule pressure of the IVC would not affect the geometry of the higher pressured AAA. However, it would be interesting to see if the IVC could affect the geometry of the AAA when the IVC was interacting with the ILT as opposed to being closer to the actual lumen of the aorta. The effect of the ILT is something that is not currently understood and this feature is being further researched.

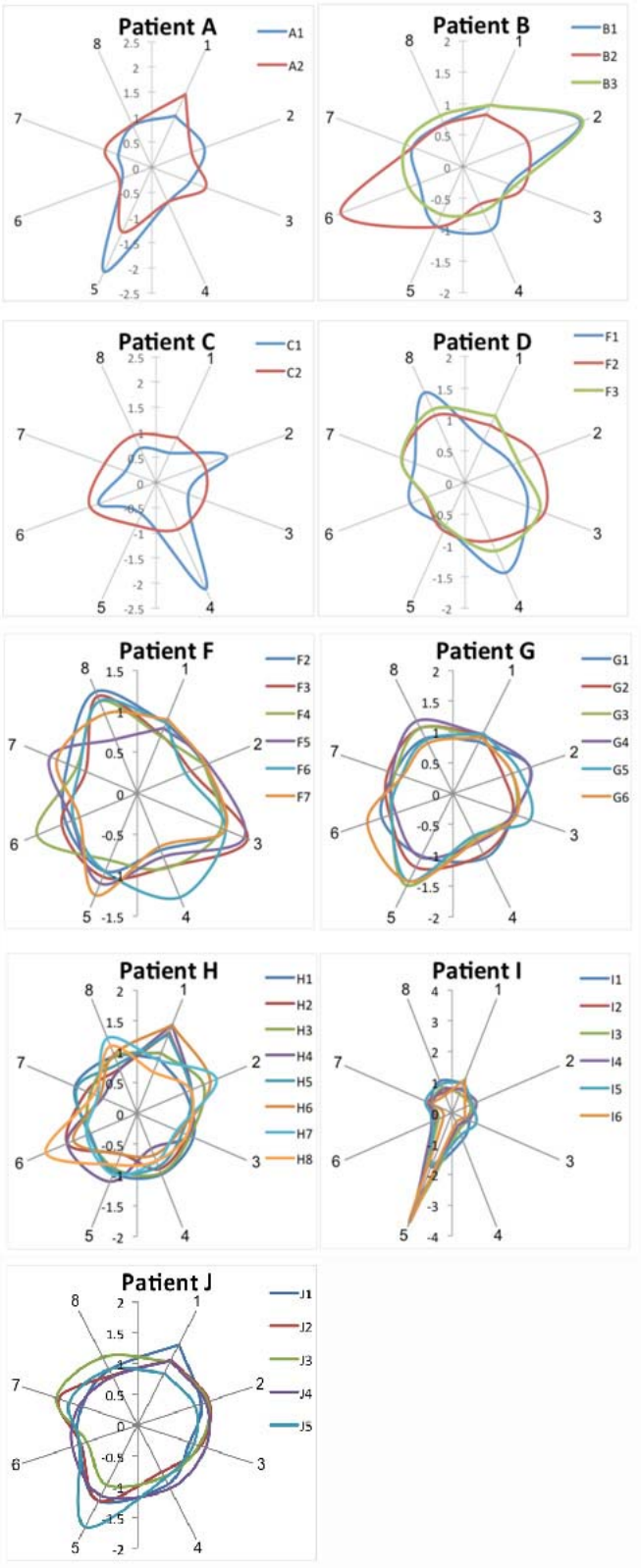

Figure 7. Radius of curvature of selected patient's scans. The radius of curvature (R*) is normalized by the mean value of each patient.

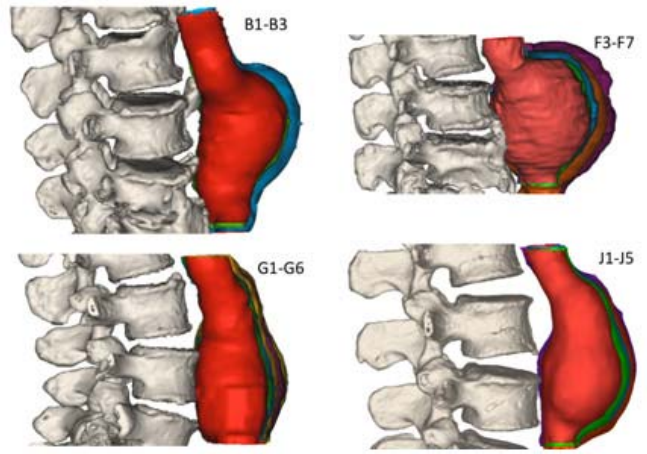

Figure 8. View of the right side of the overlaid longitudinal AAA disease progression for patient B (B1 – B3), F (F3-F7), G (G1 – G6), and J (J1 – J5). The overlapped images show the colors in the order of the CT scans from red, green, blue, orange, purple, and yellow, respectively.

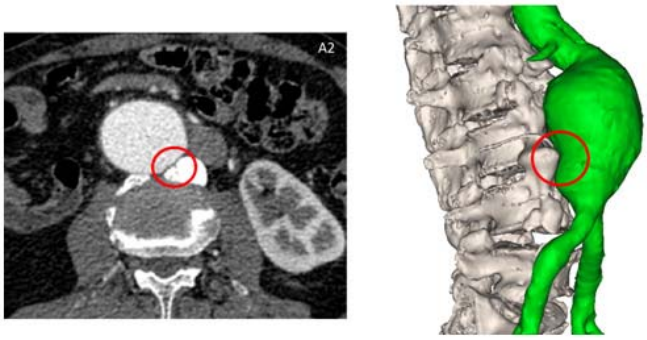

Figure 9. Ossification contact from patient A (A2)

The vertebral column can affect the circumferential shape of an aneurysmal wall, which can lead to substantially different AAA growth & remodeling, especially with regard to accelerated tissue degradation or biological adaptation induced by mechanical forces. An anteriorly growing aneurysmal wall may grow relatively unconstrained, while a posteriorly growing AAA presents additional considerations. Rupture of AAA tends to be located on the posterior or posterolateral side [6,27], which may partly be due to the vertebral column. This corresponds well with our study since it is thought that the areas of highest stress concentration would be between sections of high radii of curvature and sections of low radii of curvature (sections 4-6). It is also possible that during AAA expansion, the AAA is globally repelled away from the spine by induced spine-AAA contact forces, resulting in more curvature on the opposite or anterior side of AAA. Since the aorta is essentially fixed above and below the AAA, this migration would cause an increase in curvature on the opposite or anterior side of the AAA, resulting in an elevation in the resisting forces generated by AAAs anterior wall tension [28]. Consequently in this case, AAA takes a configuration that looks like it is being compressed from both posterior (from the spine) and anterior sides.

We speculate that the left renal vein can serve as an anchor to the infrarenal AAA during expansion. It may also be possible that the physical constraint of the left renal vein over the vessel and the tethering of the renal arteries provide a strong confinement, or an anchor at the region of the aorta, below which the aorta gradually bends as the lesion progresses, leading to some degree of tortuosity. The spine and the IVC may also affect tortuosity by interacting with the AAA. Fillinger et al. reported from 259 patients (122 ruptured and elective repair) that the most significant geometrical variables that affected the likelihood of rupture were aortic tortuosity, diameter asymmetry, and current smoking [27]. Although aortic tortuosity and diameter asymmetry may be not the only factors affected by interacting surrounding tissues, they may eventually induce AAA rupture due to the generation of higher reaction forces. Similarly, an FEA analysis suggests that an AAA that has a highly asymmetric shape displays increased wall stress compared to a symmetrically shaped AAA.

Calcification commonly occurs in AAAs and also plays an important role in the biomechanics of AAA [22,29–32]. Since areas of calcification have higher stiffness, the wall stress distribution changes, which may lead to adverse effects. Speelman et al. used FEA to see that peak wall stress was higher in areas of calcification [22]. Although calcification was found in nine out of the ten patients in this study, the calcification was not as severe when compared to other studies [22,31]. All patients in this study with ossification also had calcification, which may suggest some association, but this is not concrete.

FEA models are used to estimate AAA's wall stress based on medical images. While some of these models assume a nonlinear constitutive model of vascular wall to evaluate its stress distribution at a fixed point in time [7,17,22,33,34], other efforts have been done to not only calculate AAA wall stress distribution during its growth, but also account for the evolution of vascular wall material properties [35,36]. Some latter FEA studies have been done regarding the ability of arterial wall to adapt with its mechanical environment [37–39]. To better understand the role of mechanical stimuli in vascular adaption, several vascular G&R models have been introduced within finite element framework [12,40–45]. These models are capable of estimating the mechanical state and microstructural properties of a vascular wall's constituents at each time based on their microstructural information at a given previous time. In addition, some FEA based research has been done on the effect of surrounding tissues such as the aorta's branches [46] or adipose tissues [47] on a thoracic aorta's stability and wall stress distribution. Based on the above FEA based analyses, there is a similar need for an artery's 3-D geometric reconstruction for computational purposes.

The current paper is only an initial study using longitudinal patient scans; thus, there are clear limitations. The effects of the surrounding tissues on the AAA were somewhat subjective since segmentation was done by hand. Additionally, the ILT was not distinguished from the lumen, and the degree of interaction between the AAA and surrounding tissues may be dependent on whether this interaction is with the ILT or closer to the lumen. Consequently, further work is necessary in order to accurately portray these tissues in FEA and G&R models. The current paper provides radiologic evidence that surrounding tissues play a clear role in the growth of AAA. The next step would be to provide a solid, immobile posterior barrier that represents the spine in future FEA and G&R models. Additional future steps would be to quantify the effect of the ILT, left infrarenal vein, and IVC in an effort to incorporate these factors into models. With the increase in personalized medicine and the use of individual CT scans to predict the rupture rate, individualized effects of surrounding tissues such as osteophytes could lead to a more accurate model. The current paper's results provide an opportunity for improvement of FEA and G&R models.

CONCLUSION

With the incorporation of additional factors, such as the effects of surrounding tissue, into FEA and G&R models, more accurate simulations can be performed. By developing morphological features validated by mechanical models, medical professionals can better understand the state of stress in an AAA without actually having to analyze stress. Understandably, physicians would be weary of switching to a newer, complicated method of determining rupture risk (FEA and G&R models) when, currently, they can easily look at the size of the AAA to determine the best course of treatment. However, with further development of these models, prioritization of important variables leading to the creation of a simpler, user-friendly model that uses patient-specific CT scans is not out the question. This would minimize the work of the physician and lead to better estimates of patient-specific rupture risk, leading to a decrease in mortality from AAA rupture.

Acknowledgement
Research reported in this publication was supported by the National Heart, Lung, and Blood Instintute of the National Institutes of Health (R01HL115185 and R21HL113857) and National Science Foundation (CMMI-1150376). The contents of solely the responsibility of the authors and does not necessarily represent the official views of the National Instututes of Health.

[1] H.C. Veldenz, T.H. Schwarcz, E.D. Endean, D.B. Pilcher, P.B. Dobrin, G.L. Hyde, Morphology predicts rapid growth of small abdominal aortic aneurysms, Ann Vasc Surg. 8 (1994) 10–13. doi:10.1007/BF02133400.

[2] D. Drury, J.A. Michaels, L. Jones, L. Ayiku, Systematic review of recent evidence for the safety and efficacy of elective endovascular repair in the management of infrarenal abdominal aortic aneurysm, British Journal of Surgery. 92 (2005) 937–946. doi:10.1002/bjs.5123.

[3] Long-term outcomes of immediate repair compared with surveillance of small abdominal aortic aneurysms, New England Journal of Medicine. 346 (2002) 1445–1452. doi:10.1056/NEJMoa013527.

[4] F.A. Lederle, S.E. Wilson, G.R. Johnson, D.B. Reinke, F.N. Littooy, C.W. Acher, et al., Immediate repair compared with surveillance of small abdominal aortic aneurysms, New England Journal of Medicine. 346 (2002) 1437–1444.

[5] J.T. Powell, L.C. Brown, J.F. Forbes, F.G. Fowkes, R.M. Greenhalgh, C.V. Ruckley, et al., Final 12-year follow-up of surgery versus surveillance in the UK Small Aneurysm Trial, Br. J. Surg. 94 (2007) 702–708.

[6] R.C. Darling, C.R. Messina, D.C. Brewster, L.W. Ottinger, Autopsy study of unoperated abdominal aortic aneurysms. The case for early resection., Circulation. 56 (1977).

[7] M.F. Fillinger, M.L. Raghavan, S.P. Marra, J.L. Cronenwett, F.E. Kennedy, In vivo analysis of mechanical wall stress and abdominal aortic aneurysm rupture risk, J Vasc Surg. 36 (2002) 589–597.

[8] T.C. Gasser, M. Auer, F. Labruto, J. Swedenborg, J. Roy, Biomechanical rupture risk assessment of abdominal aortic aneurysms: model complexity versus predictability of finite element simulations, Eur J Vasc Endovasc Surg. 40 (2010) 176–185. doi:10.1016/j.ejvs.2010.04.003.

[9] A. Maier, M.W. Gee, C. Reeps, J. Pongratz, H.-H. Eckstein, W.A. Wall, A comparison of diameter, wall stress, and rupture potential index for abdominal aortic aneurysm rupture risk prediction, Ann Biomed Eng. 38 (2010) 3124–3134. doi:10.1007/s10439-010-0067-6.

[10] A.K. Venkatasubramaniam, M.J. Fagan, T. Mehta, K.J. Mylankal, B. Ray, G. Kuhan, et al., A comparative study of aortic wall stress using finite element analysis for ruptured and non-ruptured abdominal aortic aneurysms, Eur J Vasc Endovasc Surg. 28 (2004) 168–176. doi:10.1016/j.ejvs.2004.03.029.

[11] D.A. Vorp, M.L. Raghavan, M.W. Webster, Mechanical wall stress in abdominal aortic aneurysm: influence of diameter and asymmetry, Journal of Vascular Surgery. 27 (1998) 632–639.

[12] P.N. Watton, N.A. Hill, M. Heil, A mathematical model for the growth of the abdominal aortic aneurysm, Biomech Model Mechanobiol. 3 (2004) 98–113. doi:10.1007/s10237-004-0052-9.

[13] B.J. Doyle, A. Callanan, P.E. Burke, P.A. Grace, M.T. Walsh, D.A. Vorp, et al., Vessel asymmetry as an additional diagnostic tool in the assessment of abdominal aortic aneurysms, Journal of Vascular Surgery. 49 (2009) 443–454.

[14] E. Georgakarakos, C.V. Ioannou, Y. Kamarianakis, Y. Papaharilaou, T. Kostas, E. Manousaki, et al., The role of geometric parameters in the prediction of abdominal aortic aneurysm wall stress, European Journal of Vascular and Endovascular Surgery. 39 (2010) 42–48.

[15] G. Giannoglou, G. Giannakoulas, J. Soulis, Y. Chatzizisis, T. Perdikides, N. Melas, et al., Predicting the risk of rupture of abdominal aortic aneurysms by utilizing various geometrical parameters: Revisiting the diameter criterion, ANGIOLOGY. 57 (2006) 487–494. doi:10.1177/0003319706290741.

[16] G. Martufi, E.S. Di Martino, C.H. Amon, S.C. Muluk, E.A. Finol, Three-dimensional geometrical characterization of abdominal aortic aneurysms: image-based wall thickness distribution, J Biomech Eng. 131 (2009) 061015. doi:10.1115/1.3127256.

[17] M.L. Raghavan, D.A. Vorp, M.P. Federle, M.S. Makaroun, M.W. Webster, Wall stress distribution on three-dimensionally reconstructed models of human abdominal aortic aneurysm, Journal of Vascular Surgery. 31 (2000) 760–769.

[18] J. Shum, G. Martufi, E. Di Martino, C.B. Washington, J. Grisafi, S.C. Muluk, et al., Quantitative assessment of abdominal aortic aneurysm geometry, Ann Biomed Eng. 39 (2011) 277–286. doi:10.1007/s10439-010-0175-3.

[19] D.H.J. Wang, M.S. Makaroun, M.W. Webster, D.A. Vorp, Effect of intraluminal thrombus on wall stress in patient-specific models of abdominal aortic aneurysm, Journal of Vascular Surgery. 36 (2002) 598–604.

[20] M. Xenos, S. Rambhia, Y. Alemu, S. Einav, J. Ricotta, N. Labropoulos, et al., Mimics based image reconstruction augments diagnosis and management of vascular pathologies: a study of ruptured abdominal aortic aneurisms, Mimics Innovation Awards. (2009).

[21] D. Bluestein, K. Dumont, M. De Beule, J. Ricotta, P. Impellizzeri, B. Verhegghe, et al., Intraluminal thrombus and risk of rupture in patient specific abdominal aortic aneurysm - FSI modelling, Comp. Methods in Biomechanics & Biomedical Eng. 12 (2009) 73–81. doi:10.1080/10255840802176396.

[22] L. Speelman, A. Bohra, E.M.H. Bosboom, G.W.H. Schurink, F.N. van de Vosse, M.S. Makaroun, et al., Effects of wall calcifications in patient-specific wall stress analyses of abdominal aortic aneurysms, Journal of Biomechanical Engineering. 129 (2007) 105–109.

[23] B. Wolters, M.C.M. Rutten, G.W.H. Schurink, U. Kose, J. De Hart, F.N. Van De Vosse, A patient-specific computational model of fluid–structure interaction in abdominal aortic aneurysms, Medical Engineering & Physics. 27 (2005) 871–883.

[24] J.H. Leung, A.R. Wright, N. Cheshire, J. Crane, S.A. Thom, A.D. Hughes, et al., Fluid structure interaction of patient specific abdominal aortic aneurysms: a comparison with solid stress models, BioMedical Engineering OnLine. 5 (2006) 33.

[25] Y. Papaharilaou, J.A. Ekaterinaris, E. Manousaki, A.N. Katsamouris, A decoupled fluid structure approach for estimating wall stress in abdominal aortic aneurysms, Journal of Biomechanics. 40 (2007) 367–377.

[26] A. Dupay, Investigation of surface evolution for abdominal aortic aneurysms interacting with surrounding tissues, Master Thesis at Michigan State University. (2012).

[27] M.F. Fillinger, J. Racusin, R.K. Baker, J.L. Cronenwett, A. Teutelink, M.L. Schermerhorn, et al., Anatomic characteristics of ruptured abdominal aortic aneurysm on conventional CT scans: Implications for rupture risk, J. Vasc. Surg. 39 (2004) 1243–1252. doi:10.1016/j.jvs.2004.02.025.

[28] M. Farsad, S. Zeinali-Davarani, J. Choi, S. Baek, A computational approach to investigate the effect of spine as a constraint on abdominal aortic aneurysm growth and remodeling, Journal of Biomechanical Engineering. in print (n.d.).

[29] S. de Putter, F.N. van de Vosse, M. Breeuwer, F.A. Gerritsen, Local influence of calcifications on the wall mechanics of abdominal aortic

aneurysm, (2006) 61432E–61432E. doi:10.1117/12.650480.

[30] J.S. Lindholt, Aneurysmal wall calcification predicts natural history of small abdominal aortic aneurysms, Atherosclerosis. 197 (2008) 673–678. doi:10.1016/j.atherosclerosis.2007.03.012.

[31] A. Maier, M.W. Gee, C. Reeps, H.-H. Eckstein, W.A. Wall, Impact of calcifications on patient-specific wall stress analysis of abdominal aortic aneurysms, Biomech Model Mechanobiol. 9 (2010) 511–521. doi:10.1007/s10237-010-0191-0.

[32] C. Reeps, M. Gee, A. Maier, M. Gurdan, H.-H. Eckstein, W.A. Wall, The impact of model assumptions on results of computational mechanics in abdominal aortic aneurysm, J. Vasc. Surg. 51 (2010) 679–688. doi:10.1016/j.jvs.2009.10.048.

[33] P. Rissland, Y. Alemu, S. Einav, J. Ricotta, D. Bluestein, Abdominal aortic aneurysm risk of rupture: patient-specific FSI simulations using anisotropic model, Journal of Biomechanical Engineering. 131 (2009) 031001.

[34] A. Dorfmann, C. Wilson, E.S. Edgar, R.A. Peattie, Evaluating patient-specific abdominal aortic aneurysm wall stress based on flow-induced loading, Biomech Model Mechanobiol. 9 (2010) 127–139. doi:10.1007/s10237-009-0163-4.

[35] S. Zeinali-Davarani, A. Sheidaei, S. Baek, A finite element model of stress-mediated vascular adaptation: application to abdominal aortic aneurysms, Computer Methods in Biomechanics and Biomedical Engineering. 14 (2011) 803–817. doi:10.1080/10255842.2010.495344.

[36] S. Zeinali-Davarani, S. Baek, Medical image-based simulation of abdominal aortic aneurysm growth, Mechanics Research Communications. 42 (2012) 107–117. doi:10.1016/j.mechrescom.2012.01.008.

[37] M.J. Mulvany, Vascular growth in hypertension, Journal of Cardiovascular Pharmacology. 20 (1992) S7–11.

[38] A.G. Driss, J. Benessiano, P. Poitevin, B.I. Levy, J.-B. Michael, Arterial expansive remodeling induced by high flow rates, Am. J. Physiol. 272 (1997) H851–H858.

[39] Z.S. Jackson, D. Dajnoweiec, A.I. Gotlieb, B.L. Langille, Partial off-loading of longitudinal tension induces arterial tortuosity, Arterioscl. Thromb. Vasc. Biol. 25 (2005) 957–962.

[40] S. Baek, K.R. Rajagopal, J.D. Humphrey, A theoretical model of enlarging intracranial fusiform aneurysms, ASME Journal of Biomedical Engineering. 128 (2006) 142–149.

[41] M. Kroon, G.A. Holzapfel, A model for saccular cerebral aneurysm growth by collagen fibre remodelling, Journal of Theoretical Biology. 247 (2007) 775–787.

[42] C.A. Figueroa, S. Baek, C.A. Taylor, J.D. Humphrey, A computational framework for fluid-solid-growth modeling in cardiovascular simulations, Computer Methods in Applied Mechanics and Engineering. 198 (2009) 3583–3602.

[43] P.N. Watton, N.B. Raberger, G.A. Holzapfel, Y. Ventikos, Coupling the hemodynamic environment to the evolution of cerebral aneurysms: computational framework and numerical examples, J Biomech Eng. 131 (2009) 101003. doi:10.1115/1.3192141.

[44] I. Hariton, G. deBotton, T.C. Gasser, G.A. Holzapfel, Stress-modulated collagen fiber remodeling in a human carotid bifurcation, J. Theor. Biol. 248 (2007) 460–470. doi:10.1016/j.jtbi.2007.05.037.

[45] M. Kroon, G.A. Holzapfel, A theoretical model for fibroblast-controlled growth of saccular cerebral aneurysms, J. Theor. Biol. 257 (2009) 73–83. doi:10.1016/j.jtbi.2008.10.021.

[46] P. Moireau, N. Xiao, M. Astorino, C.A. Figueroa, D. Chapelle, C.A. Taylor, et al., External tissue support and fluid-structure simulation in blood flows, Biomech Model Mechanobiol. 11 (2012) 1–18. doi:10.1007/s10237-011-0289-z.

[47] J. Kim, B. Peruski, C. Hunley, S. Kwon, S. Baek, Influence of surrounding tissues on biomechanics of aortic wall., International Journal of Experimental and Computational Biomechanics. 2 (2013) 105–117. doi:10.1504/IJECB.2013.056516.